UDC 654.165:621.395.742 **doi: 10.32620/reks.2023.2.06**

Hubbul WALIDAINY, Nawal NASHIRAH, Ramzi ADRIMAN,
Yuwaldi AWAY, Nasaruddin NASARUDDIN*

Universitas Syiah Kuala, Banda Aceh, Indonesia

STATISTICAL CHANNEL MODEL FOR 6G COMMUNICATION NETWORKS IN BANDA ACEH CITY

Wireless technology is expected to undergo considerable transformation because of the numerous services offered by 6G communication networks, which virtually entirely encompass every part of everyday life and use a variety of devices. Channel modeling is an essential factor in designing 6G communication networks. To meet the channel requirements of future 6G communication networks, it is crucial to measure the channel to consider path loss, multi-band, fading, blocking effect, multipath clustering, transmitter, and receiver moving speed/direction/time. ***The goal*** *of this paper is to design and evaluate a 6G communication network in Banda Aceh City using a statistical channel model. The channel model is associated with environmental conditions such as rainfall and humidity.* ***The method*** *is then based on computer simulation using the NYUSIM simulator to complete the channel modeling using an operating frequency of 95 GHz with a bandwidth of 800 MHz. In the simulator, the designed 6G channel model is evaluated in both line-of-sight (LOS) and non-line-of-sight (NLOS) network environments. In addition, the designated network parameters, such as the coverage area, angle of arrival (AoA), angle of departure (AoD), and power delay profile (PDP), are simulated.* ***The results****, at AoA, the value of received power for LOS conditions ranges from -86 dBm to -101 dBm, while the value for NLOS conditions ranges from -91 dBm to -111 dBm. Under LOS conditions, the received power for AoD ranges from -86 dBm to -101 dBm, whereas under NLOS conditions, it ranges from -91 dBm to -111 dBm. In the omnidirectional PDP, the pathloss value for the LOS condition is 99.8 dB and the delay is 17.9 ns, while the pathloss value for the NLOS condition is 104.2 dB with a delay of 28.1 ns. For the directional PDP, the LOS condition yields a path loss of 106.4 dB and a delay of 2.9 ns, while the NLOS condition yields a path loss of 110.5 dB and a delay of 3 ns.* ***Conclusions****. The simulation indicated that the AoA, AoD, and PDP in terms of received power, pathloss, and propagation delay are in acceptable conditions for a 6G network in Banda Aceh City in the two observed environments. Therefore, it is conceivable to establish a 6G network in Banda Aceh City in the future.*

Keywords*: channel model; 6G network; statistical; NYUSIM; evaluation.*

1. Introduction

Wireless communication technology is increasing in the form of cellular devices such as cell phones, iPads, laptops, and others. This wireless technology makes it easier for people to communicate or transfer data without using additional tools (such as cables) to connect the two communication devices. In addition to its conveniences, wireless technology enables users to communicate with greater flexibility and efficiency [1]. In 2021, the number of wireless telecommunications consumers in Indonesia reached 365.9 million. Compared to user data from the start of 2020, this number has increased by 2.88%. Today, telecommunications technology is indispensable and cannot be avoided. Until optimal results are achieved, equipment and infrastructure enhancements will persist. As the world's first IP-based cellular network, the fourth generation (4G) mobile communication system is being developed [2].

Using Long Term Evolution (LTE) technology, the 4G network offers speeds up to 100 Mbps. Long Term Evolution is commonly associated with this generation (LTE). This LTE network is being upgraded to LTE-Advanced as well. This network is capable of speeds up to 1 Gbps [3]. The LTE architecture was subsequently upgraded to LTE-A Pro in an effort to enhance the existing network and prepare for the introduction of the fifth generation (5G) in the future years [4]. The primary objective of LTE-A Pro is to increase the present data rates and bandwidth of mobile communication networks. Data rates are up to three times that of LTE-A (1 Gbps for LTE-A). The user experience will be substantially enhanced by optimizing the capacity, performance, and capabilities of an existing LTE-A network. For instance, the operator's LTE-A Pro bandwidth is 640 MHz, whereas its LTE-A network bandwidth is only 100 MHz [5].

Research on 5G communication networks was initiated in 2010 and expanded in the years that followed [6]. The 5G network has developed infrastructure with high standards that can be applied to various fields, including artificial intelligence, smart

© Hubbul Walidainy, Nawal Nashirah, Ramzi Adriman, Yuwaldi Away, Nasaruddin Nasaruddin, 2023

ISSN 1814-4225 (print)
ISSN 2663-2012 (online)

cities, and others. Moreover, support for the extremely high data rates of up to 10 Gbps or even higher is frequently mentioned in conjunction with 5G. This would represent a tenfold increase in data transfer rates compared to the current level. The 5G facilitates the deployment of Internet of Things (IoT) infrastructure and artificial intelligence across all industries. The 5G network launched today (marketed beginning in 2020) provides smartphones and other devices with significantly faster bandwidth and connections than the previous generation. This 5G network provides a significantly faster connection, estimated at 35.46 Gbps (approximately 35 times quicker than the 4G network). On the other hand, this 5G communication network cannot meet all future requirements for communication networks [3, 4]. In 2019, the 5G NR communication system was introduced after extensive research and testing. The 5G NR radio system is a standard for the radio access network (RAN). Initially, the control plane for non-standalone operation (NSA) relies on the 4G system. The data section and control plane in standalone operation (SA) are controlled by a disruptive 5G next-generation core (NGC) [3]. 5G NR has two frequency ranges for different application needs: Frequency Range1 (FR1) to 7.125 GHz and Frequency Range2 (FR2) for frequencies above 24.25 GHz. FR2 has an enhanced mobile broadband (eMBB) scenario, which provides Gbps communication using up to 400 MHz of bandwidth [7].

The sixth generation (6G) communication network technology is expected to surpass the previous generation of wireless cellular systems. Therefore, research has begun on the sixth generation (6G) wireless communication network, which is expected to be implemented after 2030. It is anticipated that the 6G communication network technology will be much faster than its predecessor. The 5G communication network has a data transfer rate of 20 Gbps, while the 6G communication network is anticipated to reach 1...10 Tbps. The capacity of the traffic area can exceed 1 Gbps/m^2. Compared to 5G communication networks, the spectrum efficiency of 6G networks will increase by a factor of three to five, while the energy efficiency is anticipated to increase by a factor of ten [8]. 6G communication networks are anticipated to significantly alter wireless technology. This is due to the large number of users of telecommunication services employing various devices and encompassing nearly every aspect of daily life.

Several applications, including smart society, extended reality, wireless brain-computer interaction, etc., use the 6G telecommunication network system [9]. The need for the transfer of large amounts of data at high and reliable velocities, the connection between vehicles, remote device control, and communication between devices and health services [10]. Due to the increasing number of telecommunication users every year, channel modeling is needed to optimize link performance and provide a realistic assessment of the overall performance of the communication system. Many aspects must be addressed when creating channel modeling, such as carrier frequency, bandwidth, transmitter and receiver locations, and geographic circumstances in an area to be examined [11].

6G wireless channel must be thoroughly explored to achieve a 6G communication network under the current trend, as it serves as the foundation for system design, network optimization, and evaluation of a 6G communication network's performance. Consequently, all frequency bands and scenarios for 6G wireless communication channels were thoroughly surveyed, with a focus on mmWave, THz, and optical wireless communications on all spectrum, satellite, UAV, maritime, and underwater acoustic communication channels under the global coverage scenario, and high-speed train, vehicle to vehicle, multi-input multi-output, orbital angular momentum, and IoT communication industry [8].

Channel measurement is also crucial to consider path loss, multi-band, fading, blocking effect, multipath clustering, transmitter and receiver moving speed/direction/time, and so on, to meet the channel requirements of future 6G communication networks. Meanwhile, the measured data should be processed by the channel parameter estimation algorithm [12]. Therefore, implementing a channel model is crucial in designing a wireless communication system. Furthermore, the availability of tools for designing computer-based communication systems, such as channel simulators, is beneficial for evaluating the performance of communication network systems and simulating network deployments [13].

In general, the frequency used by mmWave refers to the 30...300 GHz band, while terahertz uses the 0.1...10 THz frequency band [14]. Thus, the 100...300 GHz frequency band has some common characteristics between mmWave and terahertz, such as large bandwidth, high directivity, large path loss, blocking effect, atmospheric absorption, and more diffuse scattering. Meanwhile, mmWave is expected to be able to reach several hundred meters with data transmission speeds of up to gigabytes per second. Meanwhile, at the terahertz frequency, it is expected that the data transmission speed will reach terabytes per second with a range of up to tens of meters [8].

Researchers are continuously producing new products to drive advances in wireless communication technology. Previously considered unusable, some parts of the high frequency (frequency band) are now used for modern communication systems. To develop new devices and applications, the researchers took advantage of the frequency spectrum band between 95 GHz and 3 THz. This radio frequency range is increasingly suitable for developing and deploying new active communications services and applications [15]. In March 2019, the Federal Communications Commission (FCC) unanimously agreed to lift the electromagnetic restrictions above 95 GHz, make the 21.2 GHz spectrum available for unauthorized use, and allow investigative activity in the electromagnetic spectrum up to 3 THz. Similarly, the National Telecommunications and Information Administration (NTIA) has set a policy move toward scientific spectrum policy efficiency for future America and is encouraging NTIA to reduce the place of restrictions on spectrum beyond 95 GHz [16].

Channel modeling simulations with a frequency spectrum of 95 GHz on a 6G communication network can be done using NYUSIM software. NYUSIM is an open-source channel simulator with a MATLAB-based Graphical User Interface system developed by NYU wireless which has been researched for five years with accurate data that can be displayed in 3D dimensions. 3D statistical spatial channel modeling with modeling components to predict LOS values, large-scale path loss modeling, large-scale parameters, small-scale parameters, and delays such as cluster time delays, subpath delays, cluster power time, subpath power, spatial lobe (SL), shadow fading, omnidirectional RMS value delay, and this software has been downloaded more than 7000 times by users. Comparison of Rural Macrocell (RMa), Urban Macrocell (UMa), and Urban Microcell (UMi) scenarios with Line of Sight (LOS) and Non-Line of Sight (NLOS) conditions under different conditions of temperature, humidity, rainfall, and air pressure at an area. NYUSIM provides accurate results based on the channel impulse response, both in space and time, and is applicable to a wide range of carrier frequencies, from 500 MHz to 100 GHz, and RF bandwidth from 0 to 800 MHz [13].

This paper proposes a design of a propagation channel for a general process 6G communication network. First, this paper builds a channel model based on the parameters in the city of Banda Aceh. Furthermore, this paper conducted a simulation using NYUSIM based on these parameters. Simulations were carried out through two environmental scenarios, LOS and NLOS, to obtain the Angle of Arrival (AoA), Angle of Departure (AoD), and directional and omnidirectional PDP such as received power, path loss, and propagation delay. Finally, this paper analyzes the simulation results as a reference for implementing 6G communication networks in Banda Aceh City. The main contributions of this paper can be summarized as follows:

a) we present a design for the statistical channel model for 6G at 95 GHz in Banda Aceh City, one of Indonesia's provinces located on the equator and with a tropical climate (rainy and drier seasons only);

b) we analyze the designed 6G propagation channel link budget under LOS and NLOS conditions;

c) we simulate received power, path loss, and propagation latency to determine the viability of implementing a 6G communication system in Banda Aceh City.

2. Materials and Methods

2.1. Location Determination

The first step in designing a channel model is determining the positioning of the network to design and model the propagation channel for the 6G network. Since Banda Aceh City is one of Indonesia's urban areas, it was selected as the case study location. The site selection is required to collect data on temperature, air pressure, humidity, and precipitation as propagation channel modeling parameters. Consequently, the Urban Microcell (UMi) scenario is examined. The required data for the input parameters of the NYUSIM software simulation, such as frequency, bandwidth, air pressure, temperature, humidity, and precipitation, are gathered based on the location.

2.2. Cell scenario

As depicted in Figure 1, the coverage area of a cellular communication network system is divided into several cell areas, ranging from the smallest to the largest cells: femtocells, picocells, and microcells. The network of femtocells encompasses a home and is capable of handling communications from smartphones, televisions, and garden lights contained within the house. Additionally, the home's devices can be controlled remotely, for instance when we are out of town. Picocell networks have a greater range than femtocell networks and can reach an office building. Multiple devices can collaborate and communicate with smartphone users. For example, they turn on the lights when people are detected in a room, turn off the air conditioning when the room is empty and unoccupied, and secure the door when it is time for someone to return from work. In addition, the microcell is more comprehensive than the previous two cell varieties. In addition to managing networks within residential and commercial buildings, this network must maintain network stability for mobile devices, such as those carried by pedestrians, and motorcyclists. Heterogeneous Networks (HetNets) comprise of base station deployments of varying proportions. The HetNets is an attractive low-cost approach to meeting the expanding needs of the industry and providing consistent connectivity. HetNet is composed of small cells (SC) that facilitate the reuse of contiguous spectrum in cells [17].

ISSN 1814-4225 (print)
ISSN 2663-2012 (online)

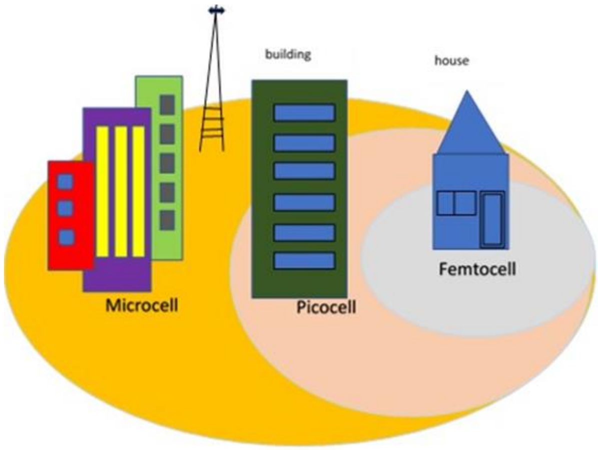

Fig. 1. Illustration of network handled by microcell [18]

A new paradigm for sub-THz physical layer seeks to maximize the spectral efficiency, reduce device complexity, or find advantageous compromises. Several potential scenarios are used to evaluate the solutions provided by suitable modulation schemes and multi-antenna systems. The transmit power in the sub-THz band is typically restricted to 20...30 dB. Consequently, a low peak-to-average power ratio (PAPR) with single carrier (SC) modulation is preferable, particularly because it reflects the sub-THz channel characteristics [19].

The sixth generation (6G) mobile communication system is expected to have very high data rates with more than 100 Gbps peak data rates. The higher frequency bands are assumed to be millimeter waves, and there are terahertz waves with a wider bandwidth than 5G. Consequently, 6G requires research and development to use terahertz waves. The terahertz frequency band has a fundamental flaw: the pathloss is greater than that of the 28 GHz frequency band. To advance the 6G radio access technology suitable for the terahertz wave, it is essential to elucidate the channel characteristics of the terahertz wave and develop a channel model. This study introduces the direction of the study of 6G radio access technology for higher frequency bands and technical issues in device technology, followed by computer simulations of 100 Gbps transmission with 100 GHz bandwidth. This study's simulation utilizes a power transmission of 30 dBm [20]. Paper [21] shows the use of different transmit power ranging from 20 to 36 dBm for optimizing the position of the unmanned aerial vehicle (UAV). In [22] UAVs with mountainous scenarios, mmWave is sensitive to hilly atmospheres. Reconfigurable intelligent surfaces (RIS) with a larger surface size were employed by the 6G to increase the coverage area [23].

They created channel modeling using NYUSIM software by entering fixed parameters such as frequency, bandwidth, air pressure, temperature, humidity, and rainfall and changing parameters such as BTS height, distance from the transmitter to receiver, and barrier distance between transmitter and receiver. Using this parameter, the simulation results are modified to reflect the characteristics of the City of Banda Aceh, as determined by the Central Bureau of Statistics of the City of Banda Aceh. This channel modeling will use an outdoor-to-outdoor propagation model with an urban microcell (UMi) scenario to monitor the transmitter and receiver. The selection of the UMi scenario can increase channel capacity so that users use the channel more effectively and transmission power is manageable due to the proximity of the coverage area. In the UMi scenario, 10 m antenna heights are used. The receiving antenna has a height of 1 m, the transmitter-to-receiver distance begins at 10 m, and the signal is in LOS and NLOS conditions.

Figure 2 depicts the proposed cell scenario, which includes four options for scenario-indicating parameters based on the propagation channel parameters: urban microcell (UMi), urban macrocell (UMa), rural macrocell (RMa), and indoor hotspot (InH). For instance, selecting "InH" will increase the carrier frequency range from 0.5...100 GHz to 0.5...150 GHz (for outdoor scenarios). Options for distance range from "Standard (10...500 m)" to "Indoor (5...50 m)," and the maximum base station height ranges from 150 m (in outdoor scenarios) to 3 m.

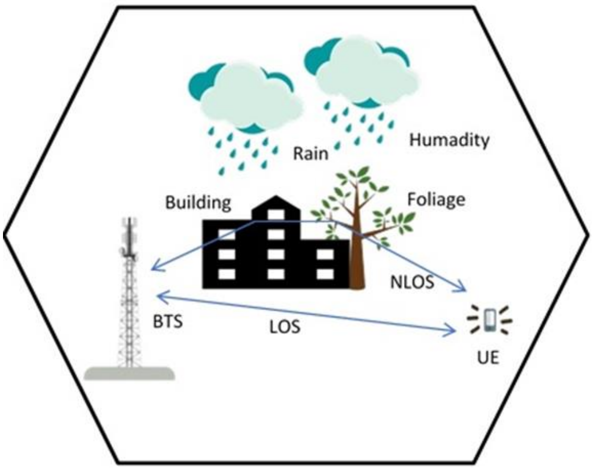

Fig. 2. Cell scenario

2.3. Environment

Two selectable parameters indicate the environment: the line of sight (LOS) or non-line of sight (NLOS), as shown in Figure 2. The LOS condition refers to the transmitting and receiving antenna located in one line of sight in a barrier-free area, or there are no obstructions between the two antennas. Meanwhile, in the NLOS condition, the path between the sender and receiver is blocked by buildings, vegetation, or other obstructions, which causes the radio signal not to reach its destination directly [4]. Therefore, it is necessary to calculate the losses that occur on the path between the sender and receiver. These losses are known as pathlosses. The reference distance for free space Pathloss model with a 1 m point, there are various damping factors used in NYUSIM and expressed as [24]:

$$\mathrm{PL^{CI}}(f_c, d_{3D})[\mathrm{dB}] = \mathrm{FSPL}(f_c, 1\mathrm{m}) + \\ +10\,n\log_{10}(d_{3D}) + \mathrm{AT} + x_\sigma^{\mathrm{CI}}, \quad (1)$$

where the symbol f represents the carrier frequency in GHz, d_{3D} is the separation distance between the 3D Transmitter-Receiver, and n represents the Pathloss Exponent (PLE). AT stands for the attenuation term caused by the atmosphere, x_σ^{CI} is a zero mean Gaussian random variable with standard deviation in dB and standard deviation σ, and $\mathrm{FSPL}(f_c, 1\mathrm{m})$ for the free space pathloss in dB units at the Transmitter-Receiver separation at a distance of 1 m for the carrier frequency [13]:

$$\mathrm{FSPL}(fc, 1\mathrm{m}) = 20\log_{10}\left(\frac{4\pi fc \times 10^9}{c}\right) = \\ = 32.4[\mathrm{dB}] + 20\log_{10} f_c, \quad (2)$$

where the speed of light is denoted by c, and the frequency (symbolized by f) is in GHz. Then the AT is expressed by [24]:

$$\mathrm{AT}[\mathrm{dB}] = \alpha[\mathrm{dB/m}] \times d[\mathrm{m}], \quad (3)$$

where the symbol α is the attenuation factor in dB/m units for the varying frequency range from 1 GHz to 100 GHz, which includes the collective attenuation effect of dry air (including oxygen), water vapor, rain, and fog, while d is the separation distance between transmitter and receiver 3D.

2.4. Attenuation of Trees/Foliage

High frequency transmissions are extremely susceptible to interference. One is the environment surrounding the transmitter antenna, which consists of towering trees and dense foliage. The leaf factor on the communication link path has a significant impact on the wireless communication quality of service (QoS).

Radiation waves can undergo attenuation, scattering, diffraction, and absorption due to discrete scatterers such as leaves, limbs, branches, and tree trunks. For instance, based on the above-mentioned equation (2), the attenuation at 95 GHz is 0.78 dB.

Tree attenuation is an important factor in attenuating signals on communication lines. Tree barriers between the transmitter and receiver add extra attenuation to the signal and greatly affect the Quality of Service (QoS) of the mmWave wireless communication system. Tree attenuation presents using the following equation [24]:

$$\gamma\mathrm{Foliage}[\mathrm{dB}] = \alpha f^{\beta} D_f^{c}\,(\theta + E)^{\epsilon}, \quad (4)$$

where f (in MHz) and D_f (in meter) are carrier frequency and tree depth. At the same time, the regression parameters α, β, c, θ, E and ϵ are empirical parameters that depend on the model used in the Weissberger model and the ITU-R model. The ITU-R model has $(\theta + E)^{\epsilon} = 1$, and α, β, and c are 0.5, 0.3, and 0.6 for distances less than or equal to 400 m. Frequency range from 230 MHz to 95 GHz. Tree attenuation can be represented by [24]:

$$\gamma\mathrm{Foliage}[\mathrm{dB}] = 0.2\, f^{0.3} D_f^{0.6}, \quad (5)$$

where f is the carrier frequency in MHz and D_f is the foliage depth in meters (d < 400 m).

2.5. Simulation Parameters

The simulation was carried out on the NYUSIM version 3.0 software, as shown in Figure 3. In the NYUSIM, the channel modeling design is carried out by entering the work parameter values as in Tables 1 and 2.

In this study, the frequency used is 95 GHz, and the selected scenario is Urban Microcell. This simulation was carried out in LOS and NLOS, with an RF bandwidth of 800 MHz. The standard distance range (10...500 m) is selected for the upper limit distance of 10 m and the lower limit of 10 m. The desired transmitter power is 20 dBm, 24 dBm, 30 dBm, and 36 dBm, with a transmitter height of 10 m and a user terminal height of 1 m.

The number of selected recipient locations is "1" because it uses one recipient. For environmental conditions, a barometric pressure of 1012.3 mbar was chosen with a humidity level of 82 % and a temperature of 27 degrees Celsius. The information presented above was based on the data from the Central Statistics Agency for Banda Aceh City for January-December 2020, which represented the real environmental conditions. Table 1 shows the data for channel parameters.

In the antenna parameter section, the type of transmitter and receiver antenna array selected are Uniform Linear Array (ULA). The transmitter and receiver antenna distance is 0.5 λ, and the azimuth and elevation half-power beamwidths are set to 10°. Table 2 shows the data for the antenna parameters. Besides the above parameters, there are several default parameters by the NYUSIM simulator that cannot be modified.

ISSN 1814-4225 (print)
ISSN 2663-2012 (online)

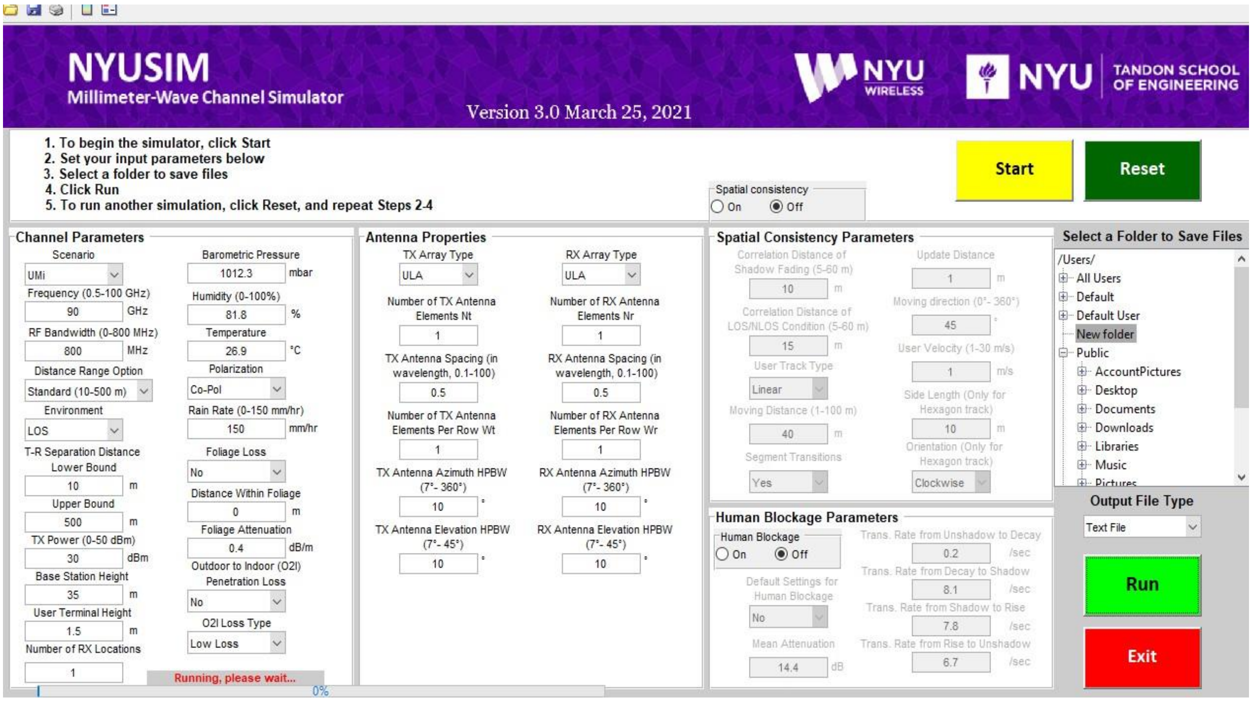

Fig. 3. NYUSIM Simulator

Table 1

Channel parameters

Parameter	Value
TX Array Type	Uniform Linear Array
RX Array Type	Uniform Linear Array
Number of TX Antenna Elements	1
Number of RX Antenna Elements	1
TX Antenna Spacing (in Wavelength 0.1-100)	0.5
RX Antenna Spacing (in Wavelength 0.1-100)	0.5
Number of TX Antenna Elements Per Row	1
Number of RX Antenna Elements Per Row	1
TX Antenna Azimuth HPBW (7°-360°)	10°
RX Antenna Azimuth HPBW (7°-360°)	10°
TX Antenna Elevation HPBW (7°-45°)	10°
RX Antenna Elevation HPBW (7°-45°)	10°

Table 2

Antenna parameters [25]

Parameter	Value
Scenario	Urban Microcell
Frequency	95 GHz [10]
RF Bandwidth	800 MHz
Distance Range Option	10 m
Environment	LOS/NLOS
TX Power	20 dBm, 24 dBm, 30 dBm [19], 36 dBm [26]
Base Station Height	10 m [27]
User Terminal Height	1 m
Number of RX Location	1
Barometric Pressure	1012,3 mbar [28]
Humidity	82 % [28]
Temperature	27°C [28]
Polarization	Co-Pol
Rain Rate	150 mm [28]
Distance Within Folliage	5 m
Foliage Attenuation	0.78 dB [29]

However, the designed network parameters are determined based on the characteristics of Banda Aceh City.

In the simulation, the results are analyzed in the form of the received power value in channel modeling. Results According to the Reference Signal Received Power (RSRP) quality standard in Table 3, the received power results in a good category starting from -70 dBm to -90 dBm, and received power in a bad condition, starting from -110 dBm to -130 dBm. After analysis, the results will be displayed in the form of graph. The results are in terms of angle of arrival (AoA), angle of departure (AoD), omnidirectional/directional PDP, small-scale PDP, and pathloss.

Table 3

RSRP [34, 35]

Level	Range
Good	-70 dBm to -90 dBm
Normal	-91 dBm to -110 dBm
Bad	-110 dBm to -130 dBm

2.6. Link Budget

A link budget combines calculations of all gain and loss values in a telecommunication transmission system. The link budget contains the components [30] that determine the signal strength level reaching the receiving side. The link budget calculation is used to determine the power level required for cellular communication and base station coverage. The link budget factors include transmitted power, antenna gain, and losses [32]. Thus, the link budget calculation can be written as follows [33]:

$$P_{RX} = P_{TX} + G - L, \quad (6)$$

where P_{RX} represents received power in dBm units, P_{TX} is transmitted power in dBm, G is gain (dBm), and L is for losses (dBm). For transmit power, it usually uses watts, so it is necessary to convert it to dBm form [36]. For the conversion process, the following method is used [25, 26]:

$$\mathrm{P_{TX}(dBm)} = 10\log(\mathrm{P_{watt}}) + 30. \quad (7)$$

The antenna gain used in the link budget has units of isotropic decibels (dBi). The standard wavelength of the $\lambda/2$ dipole antenna is 2.15 dB. While the antenna gain datasheet is expressed in dBd. Thus it is necessary to convert from dBd to dBi, in the following way [26, 27]:

$$\mathrm{dBi} = \mathrm{dBd} + 2.15. \quad (8)$$

The wave signal that propagates in free space will experience loss, so the equation for free space loss is [23, 28, 37]:

$$\mathrm{FSL_{dB}} = 32.45 + 20\log(\mathrm{d}) + 20\log(\mathrm{f}), \quad (9)$$

where FSL indicates free space loss in dB units, d is the distance in kilometers, and f is the frequency in MHz.

3. Results

3.1. Network Coverage Area

Obtaining a network's coverage area is an essential aspect of network design. Figure 4 depicts the Matlab simulation result in the 6G network coverage area in Banda Aceh city. The planned network uses a BTS with a frequency of 95 GHz. The BTS antenna is located in the center of Banda Aceh (indicated by the color red) and 20 users (indicated by the color blue). It has three distinct beam directions to cover the work area surrounding the active BTS antenna, as there are three antennas on the BTS, separated by a distance of 1,200. The area expected to be covered by the BTS is 750 meters, while the farthest user that can receive signals from the BTS is 900 meters; however, there has been a significant decrease in power at this distance.

3.2. AoA, AoD, and PDP

The designed network is simulated by considering the parameters in Tables 1 and 2, then using the NYUSIM simulator to obtain the AoA, AoD, and PDP power spectrum under LOS and NLOS environmental conditions. The simulation results are as follows.

Angle of Arrival (AoA)

AoA is the angle of the multipath component of the transmitted power arriving at the receiver. Figure 5 depicts AoA power spectra with the variation of the multipath components arriving at the receiver in a) LOS and b) NLOS environments for a 20 dB power transmission. As depicted in the figure, the midpoint is the receiving antenna, and the various multipath components (blue lines) are arbitrarily grouped into several time clusters with varying amplitudes. Afterwards, several multipath components are grouped into AoA spatial lobes. Each multipath component represents the received power, and each lobe describes the propagation route of the radio signal.

Figure 5, a is the simulation result from the AoA power spectrum under LOS, where a single spatial lobe (SL) is formed from 19 multipath components. The difference in the color on the circle represents a different received power value.

ISSN 1814-4225 (print)
ISSN 2663-2012 (online)

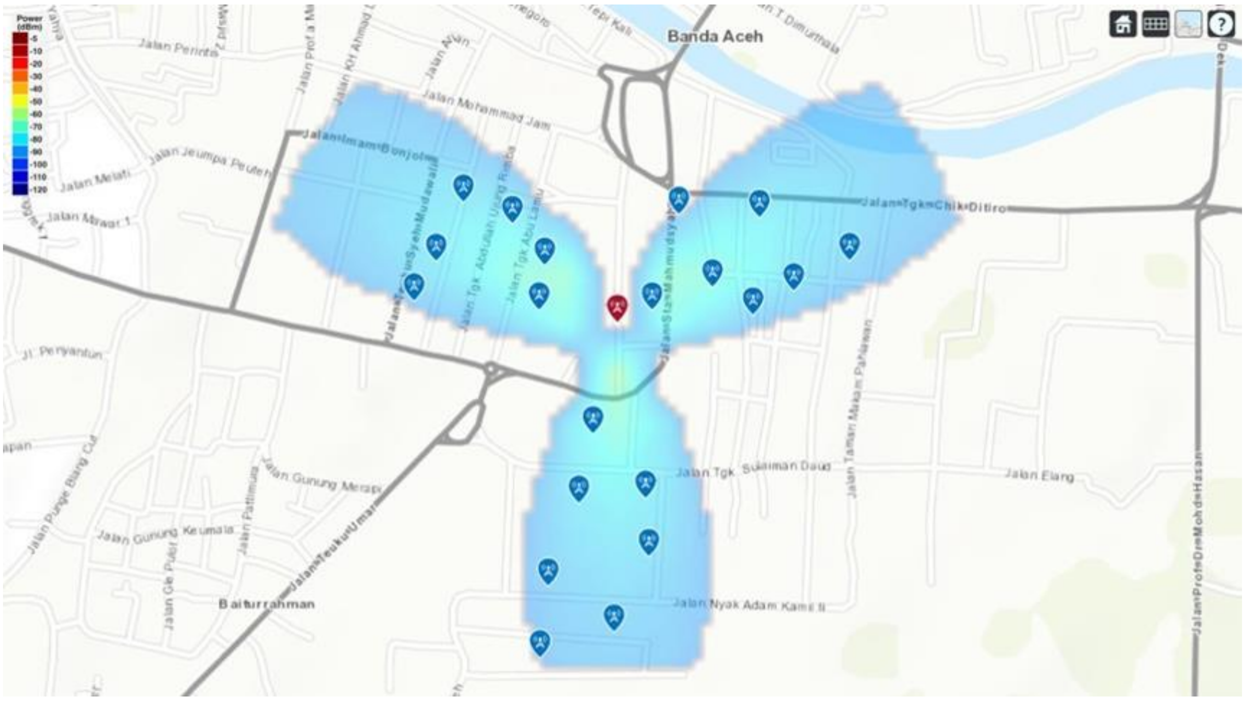

Fig. 4. The coverage area of the designed network

The yellow circle indicates the best condition with a received power value of -86 dBm, the purple circle indicates a medium condition with a value of -94 dBm, and the red circle represents the worst condition with a received power value of -101 dBm. Figure 5, b illustrates the AoA power spectrum under NLOS conditions. This demonstrates that a single SL comprises of 22 multipath components. The greatest received power is -91 dBm on the yellow circle, -101 dBm on the purple circle, and -111 dBm on the red circle.

Angel of Departure (AoD)

The AoD indicates the angle from which the signal exits. Therefore, the AoD represents the angle of the multipath/component path along which the transmitter's transmitted power travels. Figure 6 shows a spectrum of AoD power displaying the variation of the multipath component from transmitter to receiver. The midpoint is the transmitting antenna, and various multipath components (blue lines) are randomly clustered into time clusters of varying amplitudes. Afterwards, several multipath components are grouped into AoD spatial lobes. Each multipath component represents the received power, whereas each lobe represents the route of propagation.

Figure 6, a displays the AoD power spectrum for LOS conditions, which reveals the formation of two spatial lobes (SL) with 23 multipath components. The greatest received power is -86 dBm on yellow circle, -94 dBm on purple circle, and -101 dBm on red circle. Figure 6, b depicts the AoD power spectrum under NLOS

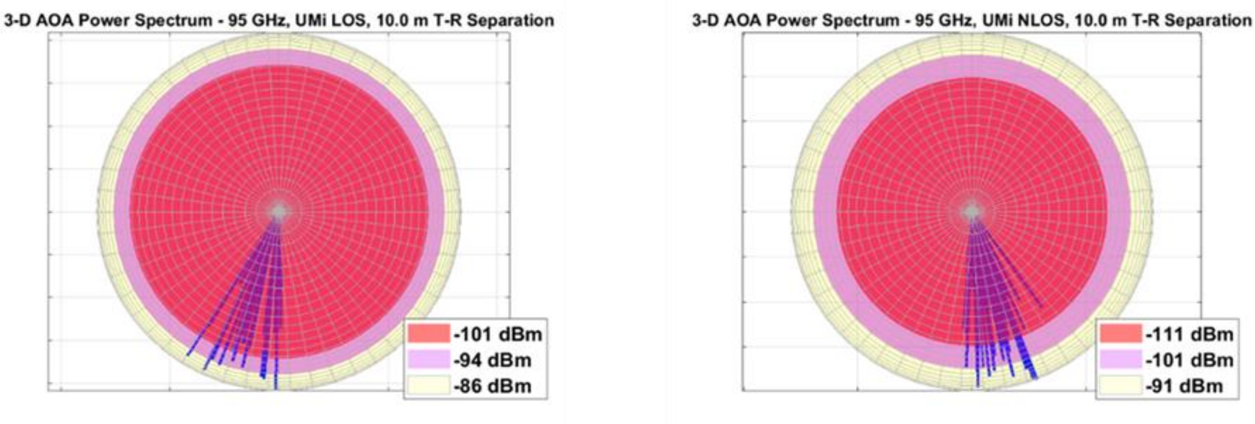

a) b)

Fig. 5. AOA power spectrum for a) LOS and b) NLOS

conditions, which revealed the formation of two spatial lobes (SL) with 29 multipath components. The greatest received power is -91 dBm on the yellow circle, -101 dBm on the purple circle, and -111 dBm on the red circle.

Power Delay Profile (PDP)

The PDP displays the received signal intensity over a multipath channel as a function of delay time. The delay time is the difference between multipath arrival travel times. There are two categories of PDP: omnidirectional and directional. Figure 7 depicts the omnidirectional PDP result that signifies the signal state level received evenly or in all directions through the multipath channel when transmitting with 20 dB of power. Multiple multipath components are clustered in time with exponentially diminishing amplitudes. In the omnidirectional PDP, signal intensity is plotted against the propagation delay for each multipath component.

Figure 7, a illustrates the outcomes of omnidirectional PDP under LOS conditions. It is determined that the received power is -70.8 dBm, the pathloss is 99.8 dB, and the delay is 17.9 ns. In the NLOS scenario depicted in Figure 7, b, the omnidirectional PDP determined the received power to be -84.2 dBm, the pathloss to be 104.2 dB, and the delay to be 28.1 ns.

The simulation result of the directional PDP is depicted in Figure 8, which depicts the level of the signal received in the direction with the maximum received power. NYUSIM searches for the optimal pointing angle among all available pointing angles using user-defined antenna parameters (HPBW azimuth and TX/RX antenna elevations) to obtain the directional PDP with the strongest reception.

Figure 8, a is the result of directional PDP in the LOS condition; the received power is -37.2 dBm, the pathloss is 106.4 dB, and the delay is 2.9 ns. Figure 8, b is the result of directional PDP NLOS, obtained the received power of -41.3 dBm, pathloss of 110.5 dB, and delay of 3 ns.

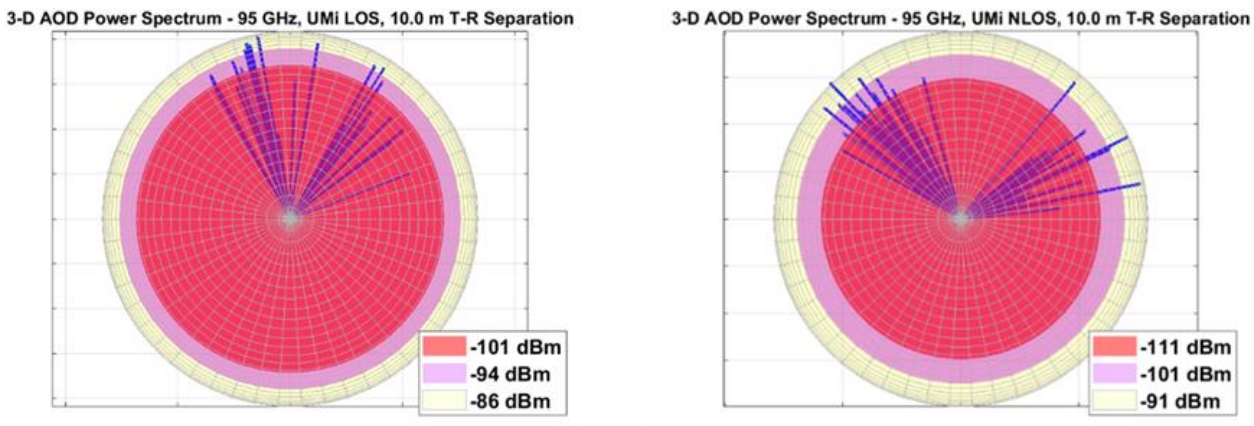

a) b)

Fig. 6. AoD power spectrum for: a) LOS and b) NLOS

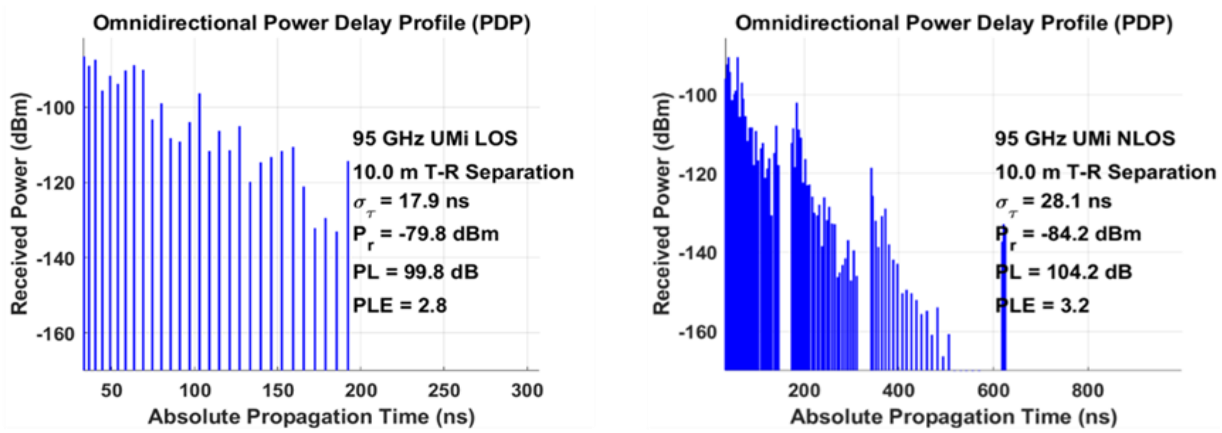

a) b)

Fig. 7. Omnidirectional PDP for a) LOS and b) NLOS

Radioelectronic and Computer Systems, 2023, No. 2(106)
ISSN 1814-4225 (print)
ISSN 2663-2012 (online)

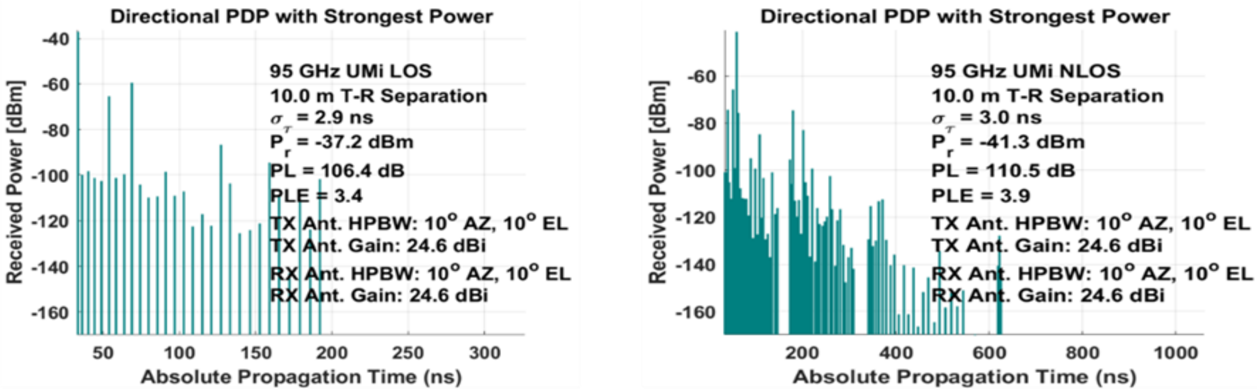

a) b)

Fig. 8. Directional PDP for a) LOS and b) NLOS

3.3. Network Evaluation

Received Power

The received signal can be divided into three categories: excellent, normal, and poor. According to [31], the ranges for excellent, normal, and poor conditions are -70 dBm to -90 dBm, -91 dBm to -110 dBm, and -110 dBm to -130 dBm, respectively. In this study, NYUSIM simulations were performed with varying transmit power and under varying conditions (LOS and NLOS). The simulation was conducted with 20 dBm, 24 dBm, 30 dBm, and 36 dBm of transmit power. Consequently, the received power generated by this simulation is highly dependent on the transmitted power.

As shown in Figure 9, at the beginning of the test, when the transmit power is 20 dBm, the receiving power under LOS conditions is -79.8 dBm. Additionally, evaluation is conducted with varying transmit capacities on the network. At 24 dBm of transmit power, the received power increased to -75.7 dBm. The transmit powers are then increased to 30 and 36 dBm, and the received powers are increased to -55.9 and -55.2 dBm, respectively. Figure 9 illustrates that in NLOS conditions, when the transmitted power is 20 dBm, the received power is -84.2 dBm. The received power was -80.2 dBm when the transmitted power was 24 dBm. Similarly, here was an increase at the 30 dBm and 36 dBm observation points, where the received powers increased to -72.9 dBm and -59.8 dBm, respectively. The optimal received power, according to the simulation results, occurs when the transmit power is 30 dBm. In both line-of-sight (LOS) and non-line-of-sight (NLOS) conditions, the greatest increase in receiving power is observed relative to other transmitters' power values. According to the ITU standard, the results obtained at 30 dBm transmit power fall within the category of acceptable received power values.

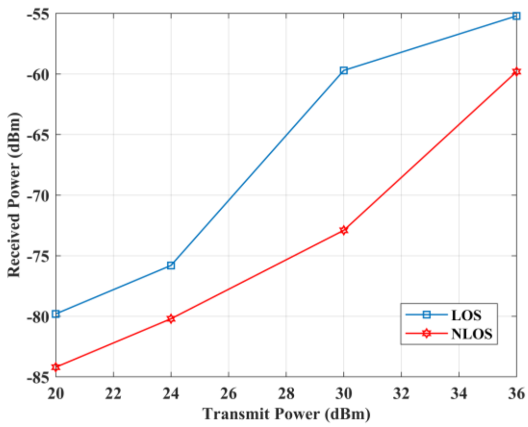

Fig. 9. Received power vs transmit power for omnidirectional PDP in LOS and NLOS

Figure 10 demonstrates that in the directional PDP, the greater the transmit power used by the base station, the greater the value of received power on the receiving side, both in the LOS and observed NLOS conditions. When the transmit power is 20 dBm, for instance, the value of the received power is -37.2 dBm. For LOS conditions, when the transmit power is 24 dBm, the value is -33.2 dBm; when the transmit power is 30 dBm, the result is -14.6 dBm; and when the transmit power is 36 dBm, the value is -10.2 dBm. These values fall within the category of excellent received power. In NLOS conditions, transmitting at 20 dBm results in a received power value of -41.3 dBm; transmitting at 24 dBm results in a received power value of -37.3 dBm. In addition, when the transmit value is 30 dBm, the received power is -25.1 dBm, and at the end point of observation, the received power is -11.3 dBm when the transmit value is 36 dBm.

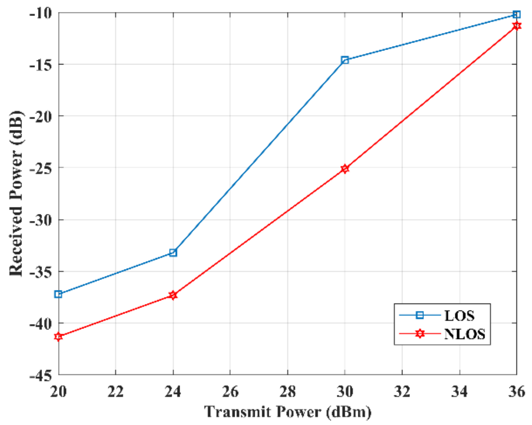

Fig. 10. Received power vs transmit power for directional PDP in LOS and NLOS

Pathloss

In the LOS condition based on omnidirectional PDP, 20 dB of transmit power is used as the starting point. Figure 11 demonstrates that the pathloss value is 99.8 dB. The same pathloss value was observed when the transmit power was 24 dB. In addition, the pathloss value decreases at 30 and 36 dBm, with values of 89.7 and 91.2 dB, respectively. In NLOS conditions, the pathloss value was 104.2 dB for transmit powers of 20 dBm and 24 dBm, respectively. At 30 dBm and 36 dBm, the pathloss value tends to decrease, with values of 102.9 dB and 95.8 dB, respectively.

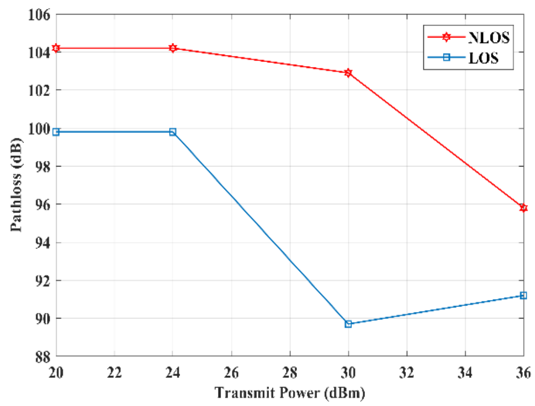

Fig. 11. Pathloss vs transmit power for omnidirectional PDP in LOS and NLOS

Consequently, there is a significant difference in simulation results between LOS and NLOS conditions, but both conditions demonstrate decreasing results. For instance, when the transmit power is 36 dBm, the pathloss value in the LOS condition slightly increases (91,2 dB) compared to the preceding situation (pathloss value of 91.2 dB). In contrast, the NLOS condition (pathloss value of 95.8 dB) continues to improve compared to the previous transmit power simulation condition.

Figure 12 illustrates the pathloss based on directional PDP in both LOS and NLOS environments. In LOS conditions, when the transmit power is 20 dBm or 24 dBm, the obtained pathloss value is 106.4 dB. Then, it decreased from 95.4 dBm to 93.9 dBm as the transmit power decreased from 30 dBm to 36 dBm. Similarly, in the NLOS scenario, the pathloss value decreases from 110.5 dB when the transmit power is 20 dBm and 24 dBm to 104.3 dB and 96.5 dB when the transmit power is 30 dBm and 36 dBm.

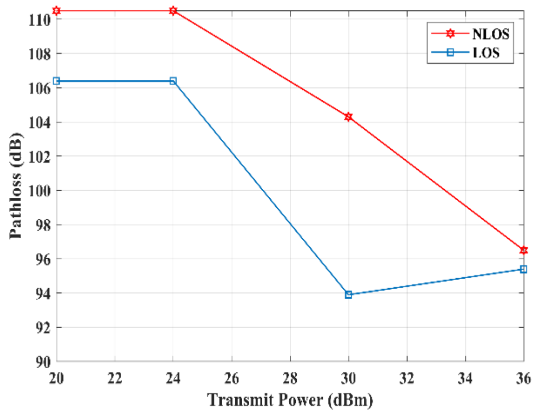

Fig. 12. Pathloss vs transmit power for directional PDP in LOS and NLOS

The trend is for the pathloss value to decrease gradually with increasing transmit power.

Propagation Delay

As depicted in Figure 13, propagation delay in both observed conditions (LOS and NLOS) tends to decrease. However, the trend of the propagation delay value decreases gradually, which is inversely proportional to the transmit power value. At transmit powers of 20 and 24 dBm, for instance, the propagation delay value is the same, with a LOS value of 17.9 ns and an NLOS value of 28.1 ns. Increasing the transmission capacity causes a decrease.

For LOS conditions, the propagation delay decreases to 15.8 ns at 30 dBm transmit power and 13.1 ns at 36 dBm transmit power. In NLOS conditions, there is a slight distinction because the decrease in propagation value at 30 dBm transmit power, which reaches 22.5 ns, is followed by a minor increase, whereas at 36 dBm transmit power, the propagation delay is 25.7 ns.

Figure 14 shows that propagation delay in the two observed conditions experienced the same thing: a

ISSN 1814-4225 (print)
ISSN 2663-2012 (online)

decrease, but this was inversely proportional to the transmit power value, which continued to increase. In LOS conditions, when the transmit power is 20 dBm, the propagation delay is 2.9 ns, and the same value is obtained when the transmit power is 24 dBm. If the transmit value is increased by 30 dBm and 36 dBm, the propagation delay value also decreases at 0.5 ns and 0.3 ns, respectively. Likewise, in NLOS conditions, the propagation delay value is 3 ns when the transmit power value is 20 dBm and at 24 dBm. When the transmit power changes to 30 dBm, the delay value also decreases by 2.8 ns. The propagation delay value decreases until it reaches 0.7 ns, although the transmit power value increases (36 dBm).

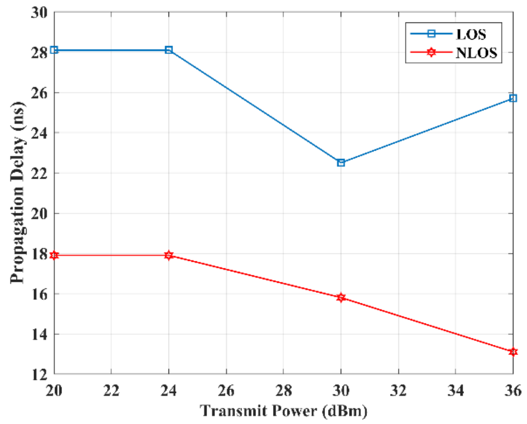

Fig. 13. Propagation delay vs transmit power for omnidirectional PDP in LOS and NLOS

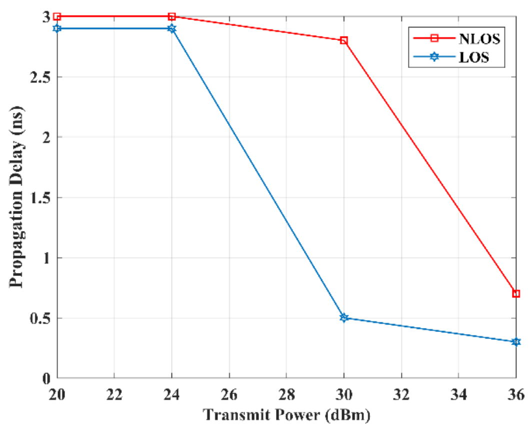

Fig. 14. Propagation delay vs transmit power directional PDP in LOS and NLOS

The result of the AoA power spectrum under LOS conditions is an SL with multipath components. Most AoA's received power is located in the purple circle (-94 dBm). This indicates that the received voltage indicates an intermediate condition and that the user can receive the signal effectively. Compared to LOS conditions, the AoA power spectrum for NLOS conditions reveals an SL with numerous multipath components. Nonetheless, the received power is typically shown in violet (-101 dBm). Thus, the signal is effectively received.

The AoD power spectrum for LOS conditions demonstrates the formation of two SLs with multipath components. The arithmetic mean of these components falls within the purple circle, indicating that the received power is moderate (-94 dBm). In NLOS conditions, the AoD power spectrum reveals the formation of 2 SL with increase in multipath components. The majority of components are located within the purple circle (-101 dBm), indicating that the value of the received power is moderate (acceptable). In LOS conditions, omnidirectional PDP achieved the highest received power, -79.8 dBm, with a pathloss of 99.8 dB.

This indicates that the value of the received power is excellent, as indicated by the yellow circle in both LOS and NLOS conditions. In addition, both LOS and NLOS have a small pathloss value and a very low delay. This paper evaluates the received power during omnidirectional PDP for four types of transmit power in the designed network, namely 20, 24, 30, and 36 dBm. There is a tendency for the received power to increase if the transmitted power is increased. When the transmit power is 30 dBm, the greatest received power is observed in both LOS and NLOS conditions.

Compared to other transmit power values, the magnitude of the increase in the received power is the greatest. The simulation results indicate that the pathloss value decreases with increasing transmit power and remains within the acceptable range. In addition, as transmit power increases, the propagation delay value tends to decrease.

The directional PDP demonstrates that the value of received power on the receiving side will increase in tandem with the base station's increasing transmit power in both NLOS and LOS conditions. In the pathloss segment, the greater the transmit power used on the sending side, the slower the value will decrease, both in LOS and NLOS conditions. The propagation latency decreased in both conditions (LOS and NLOS), but this decrease was inversely proportional to the increasing transmit power value.

Conclusions

This paper has designed and evaluated a channel model based on a statistical method for a 6G communication network by performing a simulation using the NYUSIM simulator at a frequency of 95 GHz in Banda Aceh city as the case study. First, several channel and antenna parameters related to network location have been collected to design the 6G channel network. The coverage area of the designed 6G channel model was simulated for a base station and 20 users in the network.

The result shows the beamwidth and distance link for the designed network under acceptable condition. Then, the NYUSIM simulator as a statistical model was used to evaluate the AoA, AoD, and PDP power spectrum for LOS and NLOS environments. Based on the omnidirectional PDP power spectrum, the received power and pathloss are better under LOS conditions. However, the propagation delay in NLOS conditions is better than that of LOS. In directional PDP, the received power, pathloss, and propagation delay show better results under LOS conditions. Thus, the 6G channel model has an advantage in signal transmission that faces many reflections, such as in urban areas, especially in Banda Aceh city.

Future research development. Currently, the simulation represents the initial phase of developing the network for a communication system of the 6G. Obviously, future development requires more intricate supporting parameters and more precise field testing. Today, agencies and industries working in the field of telecommunications from various parts of the globe have conducted various types of research.

6G communication system network is anticipated to fully support emerging applications, connect many devices, and provide real-time access to potent computing and storage resources. 6G networks are anticipated to be more capable, intelligent, scalable, and energy efficient than 5G networks. Moreover, the 6G communication system network must be able to ensure dependability, colossal connectivity levels, high throughput, and real-time performance.

Contributions of authors: conceptualization – **Nasaruddin Nasaruddin, Ramzi Adriman, Yuwaldi Away**; methodology – **Nasaruddin Nasaruddin, Ramzi Adriman, Yuwaldi Away, Hubbul Walidainy**; formulation of tasks – **Nasaruddin Nasaruddin**; analysis – **Nasaruddin Nasaruddin, Ramzi Adriman, Yuwaldi Away, Hubbul Walidainy**; development of model – **Hubbul Walidainy, Nawal Nashirah**; software – **Hubbul Walidainy, Nawal Nashirah**; writing – original draft preparation – **Hubbul Walidainy, Nawal Nashirah**; writing – review and editing – **Hubbul Walidainy, Ramzi Adriman, Yuwaldi Away, Nasaruddin Nasaruddin**.

All authors have read and agreed to the published version of the manuscript.

Acknowledgment. This work is funded by Doctoral dissertation research, the Ministry of Research, Technology, and Higher Education of the Republic of Indonesia, under grant no. 66/UN11.2.1/PT.01.03/DPRM /2022.

References

1. Zadereyko, O., Trofymenko, O., Prokop, Y., Loginova, N., Dyka, A. & Kukharenko, S. Research of potential data leaks in information and communication systems. *Radioelektronni i komp'uterni sistemi – Radioelectronic and computer systems*, 2022, no. 4, pp. 64-84. DOI: 10.32620/reks.2022.4.05.
2. Khatana, D. T. Study of Next Generations of Mobile Networks. *International Journal of Engineering Science and Computing*, 2020, vol. 10, iss. 2, pp. 24561-24566.
3. Giordani, M., Polese, M., Roy, A., Castor, D. & Zorzi, M. Standalone and Non-Standalone Beam Management for 3GPP NR at mmWaves. *IEEE Communications Magazine*, 2019, vol. 57, iss. 4, pp. 123-129. DOI: 10.1109/MCOM.2019.1800384.
4. Walidainy, H., Adriman, R., Away, Y. & Nasaruddin, N. Channel Modeling for 6G Communications: A Survey. *International Conference on Computer System, Information Technology, and Electrical Engineering (COSITE)*, Banda Aceh, Indonesia, 2021, pp. 1-6. DOI: 10.1109/ COSITE52651.2021.9649545.
5. A-mapat, N. & Moungnoul, P. Impact of LTE-Pro on LTE-A Network. *6th International Conference on Engineering, Applied Sciences and Technology (ICEAST)*, Chiang Mai, Thailand, 2020, pp. 1-3. DOI: 10.1109/ICEAST50382.2020.9165532.
6. Mao, Y. Analyzing the current status of global 5G research from the perspective of bibliometrics. *Journal of Physics: Conference Series*, 2021, vol. 1955, iss. 1, article no. 012050. DOI: 10.1088/1742-6596/1955/1/012050.
7. *5G; NR; User Equipment (UE) radio transmission and reception; Part 2: Range 2 Standalone (3GPP ST 38.101-2 version 15.2.0 Release 15)*. ETSI, 2018. 72 p. Available at: https://www.etsi.org/deliver/etsi_ts/138100_138199/13810102/15.02.00_60/ts_13810102v150200p.pdf. (accessed Feb. 10, 2023)
8. Wang, C.-X., Huang, J., Wang, H., Gao, X., Xiaohu, Y. & Hao, Y. 6G Wireless Channel Measurements and Models: Trends and Challenges. *IEEE Vehicular Technology Magazine*, 2020, vol. 15, iss. 4, pp. 22-32. DOI: 10.1109/MVT.2020.3018436.
9. Chowdhury, M., Shahjalal, M., Ahmed, S. & Jang, Y. M. 6G Wireless Communication Systems: Applications, Requirements, Technologies, Challenges, and Research Directions. *IEEE Open Journal of the Communications Society*, 2020, vol. 1, pp. 957-975. DOI: 10.1109/OJCOMS.2020.3010270.
10. Alsharif, M. H., Kelechi, A. H., Albreem, M. A., Chaudhry, S. A., Zia, M. S. & Kim, S. Sixth Generation (6G) Wireless Networks: Vision, Research Activities,

Challenges and Potential Solutions. *Symmetry*, 2020, vol. 12, iss. 4, article no. 676. DOI: 10.3390/sym12040676.

11. Hemadeh, I., Katla, S., El-Hajjar, M. & Hanzo, L. Dataset: Millimeter-Wave Communications: Physical Channel Models, Design Considerations, Antenna Constructions and Link-Budget. *IEEE Communications Surveys & Tutorials, 2017,* University of Southampton. [Dataset]. DOI: 10.5258/SOTON/D0344.

12. Jiang, H., Mukherjee, M., Zhou, J. & Lloret, J. Channel Modeling and Characteristics for 6G Wireless Communications. *IEEE Network*, 2021, vol. 35, iss. 1, pp. 296-303. DOI: 10.1109/MNET.011.2000348.

13. Sun, S., MacCartney, G. R. & Rappaport, T. S. A novel millimeter-wave channel simulator and applications for 5G wireless communications. *IEEE International Conference on Communications (ICC),* Paris, France, 2017, pp. 1-7. DOI: 10.1109/ICC.2017.7996792.

14. Tripathi, S., Sabu, N. V., Gupta, A. K. & Dhillon, H. S. Millimeter-wave and Terahertz Spectrum for 6G Wireless. *arXiv*, 2021, article no. 2102.10267. DOI: 10.48550/arXiv.2102.10267.

15. *FCC Opens Spectrum Horizons for New Services & Technologies.* Federal Communications Commission, 2019. Available at: https://www.fcc.gov/document/fcc-opens-spectrum-horizons-new-services-technologies-0 (accessed August 10, 2022).

16. Alsharif, M., Albreem, M., Solyman, A. & Kim, S. Toward 6G Communication Networks: Terahertz Frequency Challenges and Open Research Issues. *Computers, Materials & Continua*, 2021, vol. 66, iss. 3, pp. 2831-2842. DOI: 10.32604/cmc.2021.013176.

17. Mollel, M. S., Abubakar, A. I., Ozturk, M., Kaijage, S. F., Kisangiri, M., Hussain, S., Imran, M. A. & Abbasi, Q. H. A Survey of Machine Learning Applications to Handover Management in 5G and Beyond. *IEEE Access*, 2021, vol. 9, pp. 45770-45802. DOI: 10.1109/ACCESS.2021.3067503.

18. Jundhare, M. D. & Kulkarni, A. V. An overview and current development of femtocells in 5G technology. *IEEE International Conference on Advances in Electronics, Communication and Computer Technology (ICAECCT),* Pune, India, 2016, pp. 204-209. DOI: 10.1109/ICAECCT.2016.7942583.

19. Bicaïs, S., Doré, J.-B., Saad, M., Alawieh, M., Bader, F., Palicot, J., Corre, Y., Gougeon, G. & Faussurier, E. Wireless connectivity in the sub-THz spectrum: A path to 6G. *arXiv*, 2022, article no. 2201.06271. 30 p. DOI: 10.48550/arXiv.2201.06271.

20. Suyama, S., Okuyama, T., Kishiyama, Y., Nagata, S. & Asai, T. A Study on Extreme Wideband 6G Radio Access Technologies for Achieving 100Gbps Data Rate in Higher Frequency Bands. *IEICE Transactions on Communications*, 2021, vol. E104.B, iss. 9, pp. 992-999. DOI: 10.1587/transcom.2020FGI0002.

21. Lou, Z., Elzanaty, A. & Alouini, M.-S. Green Tethered UAVs for EMF-Aware Cellular Networks. *IEEE Transactions on Green Communications and Networking*, 2021, vol. 5, iss. 4, pp. 1697-1711. DOI: 10.1109/TGCN.2021.3102086.

22. Zhang, Z., Liu, Y., Huang, J., Zhang, J., Li, J. & He, R. Channel Characterization and Modeling for 6G UAV-Assisted Emergency Communications in Complicated Mountainous Scenarios. *Sensors*, 2023, vol. 23, iss. 11, article no. 4998. DOI: 10.3390/s23114998.

23. Fu, X., Peng, R., Liu, G., Wang, J., Yuan, W. & Kadoch, M. Channel Modeling for RIS-Assisted 6G Communications. *Electronics*, 2022, vol. 11, iss. 19, article no. 2977. DOI: 10.3390/electronics11192977.

24. Baseer, S. Impact of Human Blockage and Outdoor to Indoor Loss on 38 GHz 5G Band. *Journal of Mechanics of Continua and Mathematical Sciences*, 2020, vol. 15, iss. 9, pp. 328-343. DOI: 10.26782/jmcms.2020.09.00026.

25. *NYUSIM User Manual. Version 1.5.* New York University and NYU WIRELESS, 2017. 44 p. Available at: https://wireless.engineering.nyu.edu/wp-content/uploads/2017/03/User-Manual-for-NYUSIM_v1.5.pdf (accessed August 10, 2022).

26. Saarnisaari, H., Chaoub, A., Heikkilä, M., Singhal, A. & Bhatia, V. Wireless Terrestrial Backhaul for 6G Remote Access: Challenges and Low Power Solutions. *Frontiers in Communications and Networks*, 2021, vol. 2, article no. 710781. DOI: 10.3389/frcmn.2021.710781.

27. *LTE; 5G; Study on channel model for frequency spectrum above 6 GHz (3GPP TR 38.900 version 14.2.0 Release 14).* ETSI, 2017. 89 p. Available at: https://www.etsi.org/deliver/etsi_tr/138900_138999/138900/14.02.00_60/tr_138900v140200p.pdf. (accessed Feb. 10, 2023).

28. *Analysis of Data Needs Survey for BPS-Statistics of Banda Aceh Municipality 2021.* Available at: https://bandaacehkota.bps.go.id/publication/2021/12/23/ea277d362d04eea274ffd08c/analisis-hasil-survei-kebutuhan-data-bps-kota-banda-aceh-2021.html (accessed June 5, 2022).

29. Barb, G., Danuti, F., Ouamri, M. A. & Otesteanu, M. Analysis of Vegetation and Penetration Losses in 5G mmWave Communication Systems. *International Symposium on Electronics and Telecommunications (ISETC),* Timisoara, Romania, 2022, pp. 1-5, DOI: 10.1109/ISETC56213.2022.10009963.

30. *5G; NR; Base Station (BS) radio transmission and reception (3GPP TS 38.104 version 15.5.0 Release 15).* ETSI, 2019. 219 p. Available at: https://www.etsi.org/deliver/etsi_ts/138100_138199/138

104/15.05.00_60/ts_138104v150500p.pdf. (accessed Feb. 10, 2023).

31. Hoomod, H. K., Al-Mejibli, I. & Jabboory, A. I. Analyzing Study of Path loss Propagation Models in Wireless Communications at 0.8 GHz. *Journal of Physics: Conference Series*, 2018, vol. 1003, article no. 012028. DOI: 10.1088/1742-6596/1003/1/012028.

32. Patra, T. & Mitra, S. Link Budget Analysis for 5G Communication in the Tropical Regions. *Wireless Communications and Mobile Computing*, 2020, vol. 2020, article no. 6669965, pp. 1-9. DOI: 10.1155/2020/6669965.

33. Budalal, A. A. & Islam, Md. R. Path loss models for outdoor environment – with a focus on rain attenuation impact on short-range millimeter-wave links. *e-Prime - Advances in Electrical Engineering, Electronics and Energy*, 2023, vol. 3, article no. 100106. DOI: 10.1016/j.prime.2023.100106.

34. Radhakrishna, K. S., Yeng Seng, L., You, K. Y., Thiruvarasu, K. & Ng, S. Study of Obstacles Effect on Mobile Network and WLAN Signal Strength. *International Journal of Electronics and Telecommunications*, 2023, vol. 69, iss. 1, pp. 155-161. DOI: 10.24425/ijet.2023.144345.

35. Ghasemi, A., Abedi, A. & Ghasemi, F. *Propagation Engineering in Wireless Communications*. Springer Cham, 2016. 458 p. DOI: 10.1007/978-3-319-32783-9.

36. Qing, X. & Chen, Z. N. Omnidirectional Antennas. *Handbook of Antenna Technologies*, Singapore, Springer Singapore, 2015, pp. 1-53. DOI: 10.1007/978-981-4560-75-7_52-1.

37. Ibrahim, A. H., Alsharekh, M. F., Almanee, M. S., Al-Turki, A. S. & Islam, M. Link Budget Design for RF Line-of-Sight via Theoretical Propagation Prediction. *International Journal of Communications, Network and System Sciences*, 2019, vol. 12, no. 1, pp. 11-17. DOI: 10.4236/ijcns.2019.121002.

Надійшла до редакції 12.03.2023, розглянута на редколегії 20.05.2023

МОДЕЛЬ СТАТИСТИЧНОГО КАНАЛУ ДЛЯ ПРОЕКТУВАННЯ МЕРЕЖ ЗВ'ЯЗКУ 6G У МІСТІ БАНДА АЧЕХ

Хуббул Валідайні, Наваль Нашира, Рамзі Адріман, Ювальді Авай, Назаруддін Назаруддін

Очікується, що бездротові технології зазнають значної трансформації в результаті численних послуг, що пропонуються мережами зв'язку 6G, які практично повністю охоплюють усі аспекти повсякденного життя та використовують різні пристрої. Моделювання каналів є важливим фактором під час проєктування мереж зв'язку 6G. Щоб задовольнити вимоги до каналів майбутніх мереж зв'язку 6G, дуже важливо виміряти канал, щоб врахувати втрати на шляху, багатодіапазонність, завмирання, ефект блокування, багатопроменеву кластеризацію, швидкість/напрямок/час переміщення передавача та приймача. Метою цієї статті є проектування та оцінка мережі зв'язку 6G у місті Банда Ачех для моделі статистичного каналу. Модель каналу пов'язана з умовами навколишнього середовища, такими як опади, вологість тощо. Потім метод заснований на комп'ютерному моделюванні з використанням симулятора NYUSIM, який має завершити моделювання каналу з використанням робочої частоти 95 ГГц зі смужкою пропускання 800 МГц. У симуляторі розроблена модель каналу 6G оцінюється як у мережевих середовищах прямої видимості (LOS), так і поза прямою видимістю (NLOS). Крім того, моделюються призначені мережеві параметри, такі як зона покриття, кут приходу (AoA), кут відправлення (AoD) та профіль затримки потужності (PDP). Результати, при AoA, значення потужності, що приймається, для умов LOS знаходяться в діапазоні від -86 дБмВт до -101 дБмВт, а значення для умов NLOS знаходиться в діапазоні від -91 дБмВт до -111 дБмВт. В умовах LOS потужність, що приймається, для AoD знаходиться в діапазоні від -86 дБмВт до -101 дБмВт, тоді як в умовах NLOS вона знаходиться в діапазоні від -91 дБмВт до -111 дБмВт. У ненаправленому PDP значення втрат на трасі для умови LOS становить 99,8 дБ, а затримка становить 17,9 нс, тоді як значення втрат на трасі для NLOS становить 104,2 дБ із затримкою 28,1 нс. Для спрямованого PDP умова LOS дає втрати шляху 106,4 дБ і затримку 2,9 нс, тоді як умова NLOS дає втрати шляху 110,5 дБ і затримку 3 нс. Висновки. Моделювання показало, що AoA, AoD і PDP з точки зору прийнятої потужності, втрат на трасі і затримки розповсюдження знаходяться в прийнятному стані для мережі 6G у місті Банда Ачех у двох середах, що спостерігаються. Таким чином, у майбутньому можливе створення мережі 6G у місті Банда Ачех.

Ключові слова: модель каналу; мережа 6G; статистичний; NYUSIM; оцінка.

ISSN 1814-4225 (print)
ISSN 2663-2012 (online)

Хуббул Валідайні – магістр, керівник цифрової лабораторії, докторська програма, Інженерна школа, аспірантура, Університет Сія Куала, Банда Ачех, Індонезія.

Наваль Нашира – бакалавр, наук. співроб., каф. електротехніки та комп’ютерної інженерії, Університет Сія Куала, Банда Ачех, Індонезія.

Рамзі Адріман – д-р комп’ютерних наук та інформаційної інженерії, д-р каф. електротехніки та комп’ютерної інженерії, заступник декана інженерного факультету, Університет Сія Куала, Банда Ачех, Індонезія.

Ювальді Авай – д-р в галузі промислового комп'ютера, проф., керівник CENTRO, каф. електротехніки та комп’ютерної інженерії, Університет Сія Куала, Банда Ачех, Індонезія.

Назаруддін Назаруддін – д-р техн. наук з фізичної електроніки та інформатики, проф. каф. електротехніки та комп'ютерної інженерії, директор Управління освіти та навчання, Університет Сія Куала, Банда Ачех, Індонезія (*відповідний автор).

Hubbul Walidainy – Master degree, Head of Digital Lab., Doctoral Program, School of Engineering, Post Graduate Program, Universitas Syiah Kuala, Banda Aceh, Indonesia,
e-mail: hwalidainy@usk.ac.id, ORCID: 0000-0002-5844-9375.

Nawal Nashirah – Bachelor degree, Research Assistant, Dept. of Electrical and Computer Engineering, Universitas Syiah Kuala, Banda Aceh, Indonesia,
e-mail: nwlnshrh@gmail.com.

Ramzi Adriman – Doctoral degree in Computer Science and Information Engineering, Dr., Dept. of Electrical and Computer Engineering, Vice Dean of Engineering Faculty, Universitas Syiah Kuala, Banda Aceh, Indonesia,
e-mail: ramzi.adriman@usk.ac.id.

Yuwaldi Away – Doctoral Degree, Ph.D. in Industrial Computer, Professor, Head of CENTRO, Dept. of Electrical and Computer Engineering, Universitas Syiah Kuala, Banda Aceh, Indonesia,
e-mail: yuwaldi@usk.ac.id, ORCID: 0000-0001-6798-054X.

Nasaruddin Nasaruddin – Doctoral Degree, Doctor Eng in Physical Electronics and Informatics, Professor of Dept. of Electrical and Computer Engineering, Director of the Directorate of Education and Learning, Universitas Syiah Kuala, Banda Aceh, Indonesia,
e-mail: nasaruddin@unsyiah.ac.id, ORCID: 0000-0002-2933-1562. (*corresponding author)